Progress In Electromagnetics Research B, Vol. 91, 143–155, 2021

Diffraction Radiation Generated by a Density-Modulated Electron Beam Flying over the Periodic Boundary of the Medium Section. III. Anomalous and Resonant Phenomena

Yuriy Sirenko[1, 2], Seil Sautbekov[3, *], Nataliya Yashina[1], and Kostyantyn Sirenko[1]

Abstract—The paper is focused on the reliable analysis of the phenomena associated with the resonant and anomalous transformation of the field of a plane, density modulated electron beam, flying over the periodically rough boundary of a natural or artificial medium, in the field of bulk outgoing waves. The physical results presented here have been obtained as the result of numerical implementation of the rigorous mathematical models described in the two first papers of this series. The corresponding analytical constructions have been associated with the correct formulation of model problems and their algorithmization, with the provision of the possibility of a correct physical interpretation of the results of their numerical solution.

1. INTRODUCTION

In [1, 2], we have considered several fundamental positions related to the construction and physical analysis of the solutions to the boundary value problem

$$\begin{cases} \left[\partial_y^2+\partial_z^2+\varepsilon\left(g,k\right)\mu\left(g,k\right)k^2\right]U\left(g,k\right)=0; \quad g=\{y,z\}\in\Omega_{int} \\ \mathbf{E}_{\rm tg}\left(q,k\right),\ \mathbf{H}_{\rm tg}\left(q,k\right) \text{ are continuous when crossing } \Sigma^{\varepsilon,\mu}=\Sigma_x^{\varepsilon,\mu}\times(-\infty<x<\infty) \\ \quad \text{and virtual boundaries} \quad y=0, \quad y=-h; \quad q=\{x,y,z\} \\ U\left\{\partial_z U\right\}\left(y,l,k\right)=\exp\left(2\pi i\zeta\right)U\left\{\partial_z U\right\}\left(y,0,k\right) \quad \text{for} \quad -h\le y\le 0 \end{cases}, \tag{1a}$$

$$\begin{aligned} U\left(g,k\right) &= V_0\left(g,k\right)+U^+\left(g,k\right)=V_0\left(g,k\right)+\sum_{n=-\infty}^{\infty}U_n^+\left(g,k\right) \\ &= \exp\left(-i\Gamma_0^+y\right)\phi_0\left(z\right)+\sum_{n=-\infty}^{\infty}R_n\left(k\right)\exp\left(i\Gamma_n^+y\right)\phi_n\left(z\right); \quad g\in\overline{\mathrm{A}}, \end{aligned} \tag{1b}$$

$$U\left(g,k\right) = U^-\left(g,k\right)=\sum_{n=-\infty}^{\infty}U_n^-\left(g,k\right)=\sum_{n=-\infty}^{\infty}T_n\left(k\right)\exp\left(-i\Gamma_n^-\left(y+h\right)\right)\phi_n\left(z\right); \quad g\in\overline{\mathrm{B}}. \tag{1c}$$

This allowed us to begin to study the key energy characteristics

$$W_n^+\left(k\right)=\left|R_n\right|^2\frac{\mathrm{Re}\Gamma_n^+}{\left|\Gamma_0^+\right|}, \quad W_n^-\left(k\right)=\varepsilon^{-1}\left(k\right)\left|T_n\right|^2\frac{\mathrm{Re}\Gamma_n^-}{\left|\Gamma_0^+\right|} \tag{2}$$

Received 21 February 2021, Accepted 6 March 2021, Scheduled 10 March 2021

* Corresponding author: Seil Sautbekov (sautbek@mail.ru).

[1] Department of Diffraction Theory and Diffraction Electronics, O. Ya. Usikov Institute for Radiophysics and Electronics, National Academy of Sciences of Ukraine, 12 Academician Proskura St., Kharkiv 61085, Ukraine. [2] Department of Applied Mathematics, V. M. Karazin Kharkiv National University, 4 Svobody Sq., Kharkiv 61022, Ukraine. [3] Department of Physics and Technology, al-Farabi Kazakh National University, 71 al-Farabi Ave., Almaty 050040, Republic of Kazakhstan.

of diffraction radiation (Vavilov-Cherenkov radiation [3] or Smith-Purcell radiation [4]), generated by a plane density-modulated electron beam flying over a periodically uneven boundary $\Sigma_x^{\varepsilon,\mu}$ (see Fig. 1 in [1]) separating vacuum ($\varepsilon = \mu = 1.0$) and a dispersive (in common case) medium with material parameters $\varepsilon(k)$, $\mu(k)$; and to use, further on in the process of this study, the information about normal (or eigen) modes (which is of fundamental importance for the correct interpretation of the observed phenomena) of the periodic interface [1, 2, 5–7]. Such eigen modes are connected with nontrivial solutions to the problem in Eq. (1) for $V_0(g,k) \equiv 0$.

In Eqs. (1) and (2), $U(g,k)$ is an H_x-component of the total H-polarized ($E_x = H_y = H_z = 0$, $\partial_x = 0$) electromagnetic field $\{\mathbf{E}(g,k), \mathbf{H}(g,k)\}$, $g = \{y, z\}$ in the system 'beam — medium interface'; $V_0(g,k)$ is an H_x-component of a beam's field; $W_n^+(k)$ and $W_n^-(k)$ are the functions determining an efficiency of diffraction radiation at spatial harmonics $U_n^+(g,k)$ and $U_n^-(g,k)$, outgoing upward (in half-space occupied by vacuum) and downward (in half-space occupied by a dispersive medium) from the boundary; $\Gamma_n^+ = \sqrt{k^2 - \Phi_n^2}$, $\mathrm{Re}\Gamma_n^+ \geq 0$, $\mathrm{Im}\Gamma_n^+ \geq 0$ and $\Gamma_n^- = \sqrt{k^2\varepsilon(k)\mu(k) - \Phi_n^2}$, $\varepsilon^{-1}(k)\mathrm{Re}\Gamma_n^- \geq 0$, $\mathrm{Im}\Gamma_n^- \geq 0$ are the vertical propagation constants of these harmonics; $\phi_n(z) = l^{-1/2}\exp(i\Phi_n z)$, $n = 0, \pm 1, \pm 2, \ldots$, $\Phi_n = (n + \zeta)2\pi/l$, $\zeta 2\pi/l = \Phi_0 = k/\beta$ (with this value of Φ_0, $\mathrm{Re}\Gamma_0^+ = 0$ and $\mathrm{Im}\Gamma_0^+ > 0$, $V_0(g,k)$ is an inhomogeneous plane wave component); k and $0 < \beta < 1$ are frequency modulation and relative beam velocity; $k = 2\pi/\lambda$ is the frequency parameter; λ is a wavelength of a radiation field in a free space; l and h are period and height of the boundary $\Sigma_x^{\varepsilon,\mu} = \{g : \ y = f(z), \ -h \leq f(z) \leq 0\}$. The more detailed description of the problem in Eq. (1) is given in [1]. The choice of branches of the two-valued functions $\Gamma_n^{\pm}(k,\zeta)$ has been made and justified ibid.

In present work, we focus on anomalous and resonant phenomena in coherent diffraction radiation, which is generated by a density-modulated electron beam moving over a periodic boundary $y = f(z)$ separating an ordinary ($y > f(z)$) and ($y < f(z)$) plasma-like artificial media with the following specific frequency dispersion of permittivity and permeability:

$$\varepsilon(k) = 1 - k_\varepsilon^2/k^2 \quad \text{and} \quad \mu(k) = 1 - k_\mu^2/k^2. \tag{3}$$

As in the previous papers, the time dependence t for harmonic processes considered in this work is determined by the factor $\exp(-i\omega t)$ omitted everywhere, ω is a circular frequency. The dimensions of the SI system of all mentioned physical quantities are also omitted.

2. PRINCIPAL PECULIARITIES IN VAVILOV-CHERENKOV RADIATION

Vavilov-Cherenkov radiation (VChR) — a radiation into the lower half-space at the homogeneous plane wave $U_0^-(g,k)$ arising here — is possible only if relation (see [2])

$$\mathrm{Im}\Gamma_0^-(k) = \mathrm{Im}\sqrt{k^2\varepsilon(k)\mu(k) - \Phi_0^2} = \mathrm{Im}\sqrt{k^2\varepsilon(k)\mu(k) - k^2/\beta^2} = 0 \tag{4}$$

holds. The condition (4) may be held only in the case of binegative ($\varepsilon(k) < 0$ and $\mu(k) < 0$) or bipositive (conventional) medium. In the first case, we are dealing with a reverse VChR (the angle ϑ between the direction of the electron flow and the direction of energy transferring by the wave $U_0^-(g,k)$ is greater than $\pi/2$ [1]), in the second case — with a direct VChR ($\vartheta < \pi/2$).

Let, for the beginning, the lower half-space be filled by non-dispersive material with $\varepsilon = -0.84$, $\mu = -4.84$, and relative beam velocity $\beta = 0.89$. The resonance dip to zero of intensity of reverse VChR is clearly visible in upper fragment of Fig. 1. Here as everywhere below, $l = 2\pi$ and $f(z) = 0.5h(\cos z - 1)$. Lower fragment of Fig. 1 allows to consider the important details in the behavior of the dependencies $W_0^-(k)$ for some fixed values h that may be lost in the analysis of the overall picture of the contour plots $W_0^-(k,h) = const$. Here, function $W_0^-(k)$ vanishes at the point $k = 0.22225$ (the accuracy of calculations is determined by the sampling step of the parameter k that is equal to 0.00025), the point $k = 0.3185$ is one of the threshold points of the periodic structure [5, 6, 8, 9], each of which is uniquely associated with the manifestation of the so-called Wood's anomalies. The spatial harmonic $U_{-1}^-(g,k)$ which used to be exponentially decaying with $|y|$ increasing, when passing through this point $k = k_{-1}^- : \ \Gamma_{-1}^-(k_{-1}^-) = 0$ [1], turns into a homogeneous plane wave propagating infinitely far from the boundary $\Sigma_x^{\varepsilon,\mu}$.

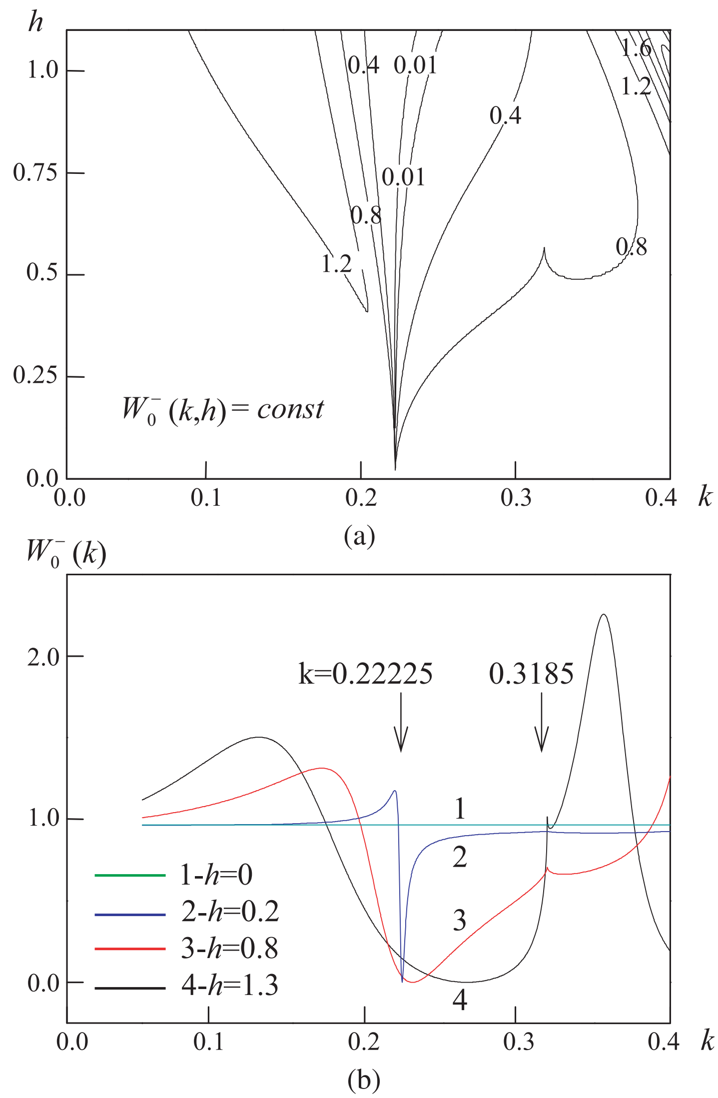

Figure 1. (a) Lines $W_0^-(k,h) = const$, characterizing the intensity of diffraction radiation into the half-space $y < f(z)$, and (b) curve $W_0^-(k)$ for various values of h : $\mu(k) = -4.84$, $\varepsilon(k) = -0.84$, and $\beta = 0.89$.

The abrupt changes in VChR intensity $W_0^-(k,h)$ in this frequency range for fixed values $h \leq 0.75$ (Fig. 2) are due to 'double resonance', whose branches split up with the growth of h. The values of W_0^- presented in the upper fragment of Fig. 2 are cut off at the level $W_0^-(k,h) = 5.0$. At sampling steps of the parameters k and h, equal to 0.00025 and 0.01, respectively, the following computed maximum values of W_0^- are: $W_0^-(k,h) \approx 321.4$ ($k = 0.44575$, $h = 0.3$) and $W_0^-(k,h) \approx 176.8$ ($k = 0.4465$, $h = 0.34$) — on the ridge I, extending to the right of the dip $W_0^-(k,h) \ll 1$; $W_0^-(k,h) \approx 145$ ($k = 0.44375$, $h = 0.17$) on the ridge II moving to the left. By decreasing the sampling step of the parameter k to 0.00001, we obtain the maximum value $W_0^-(k,h) = 519.8$ at $k = 0.44629$ and $h = 0.32$ (see Fig. 2(b)). As h increases the 'height' of the ridges I and II decreases, they become flatter. This means that the Q-factor of the corresponding resonances decreases.

In comparison with the VChR levels recorded above, the results presented in Fig. 3 look very modest. The smooth change of the curves $W_0^-(k,h) = const$ is violated here only at the threshold points $k = k_{-1}^-$ and $k = k_{-1}^+ \approx 0.4709$ [1] of the periodic structure. Moreover, this happened despite the fact that the conditions within which the effects of diffraction radiation were studied remained practically

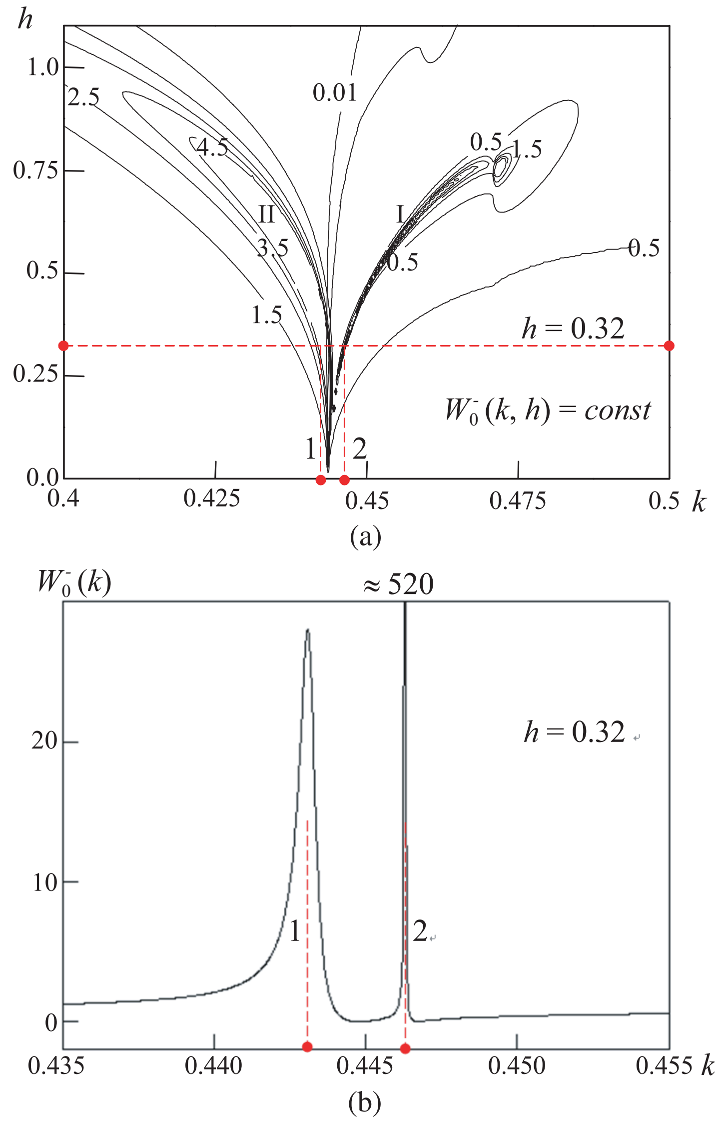

Figure 2. (a) Lines $W_0^-(k,h) = const$, characterizing the intensity of diffraction radiation into the half-space $y < f(z)$, and (b) curves $W_0^-(k)$ for values $h = 0.32$: $\mu(k) = -4.84$, $\varepsilon(k) = -0.84$, and $\beta = 0.89$.

unchanged: the same frequency range, the same electron flow velocity, the same profile of the periodic boundary, and the same absolute values of the material parameters of the medium occupying the lower half-space. But in the case considered above, this environment was binegative, while in the case of Fig. 3 — bipositive.

How does this difference result in such a significant difference in characteristics W_0^-? Representations in Eqs. (4), (6) from [2] will help us to understand this. According to these concepts, the parameters $\Phi_n(\bar{\zeta}_n^\pm) = (n + \bar{\zeta}_n^\pm)2\pi/l$, $\Gamma_n^+(\bar{\zeta}_n^\pm) = \sqrt{k^2 - \Phi_n^2(\bar{\zeta}_n^\pm)}$, $\Gamma_n^-(\bar{\zeta}_n^\pm) = \sqrt{k^2\varepsilon\mu - \Phi_n^2(\bar{\zeta}_n^\pm)}$ of eigen wave $U(g, \bar{\zeta}_n^\pm)$, guided by plane boundary $y = 0$, separating vacuum and non-dispersive medium with parameters ε and μ, meet relations

$$\Phi_n\left(\bar{\zeta}_n^\pm\right) = \pm k\sqrt{\frac{\varepsilon\left(\varepsilon - \mu\right)}{\varepsilon^2 - 1}} \quad \text{and} \quad \Gamma_n^+\left(\bar{\zeta}_n^\pm\right) = -\Gamma_n^-\left(\bar{\zeta}_n^\pm\right)\varepsilon^{-1}. \tag{5}$$

From Eq. (5) it follows that if $\mathrm{Im}\Gamma_n^\pm(\bar{\zeta}_n^\pm) = 0$, the values $\mathrm{Re}\Gamma_n^+(\bar{\zeta}_n^\pm)$ and $\varepsilon^{-1}(k)\mathrm{Re}\Gamma_n^-(\bar{\zeta}_n^\pm)$ differ in

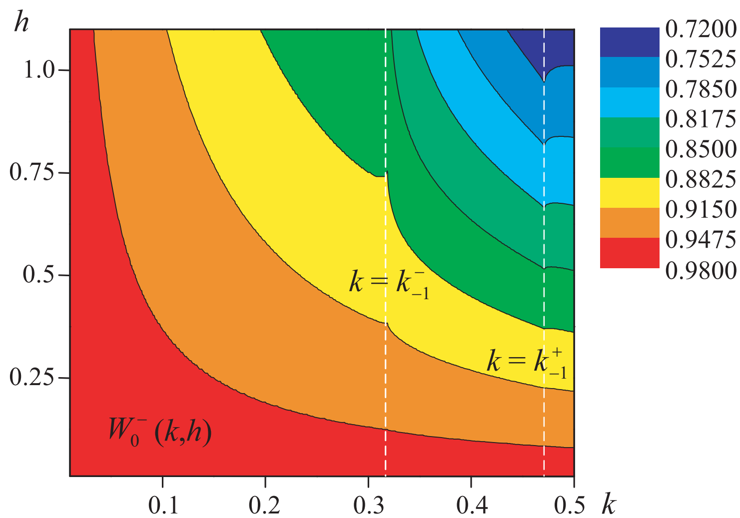

Figure 3. Intensity $W_0^-(k,h)$ of radiation into a half-space occupied by a bipositive nondispersive medium: $\mu(k) = 4.84$, $\varepsilon(k) = 0.84$, and $\beta = 0.89$.

signs, and therefore: (a) the real propagation constant $\bar{\zeta}_n^{\pm}$ cannot belong to a first (physical) sheet of the surface F_n same as for $\varepsilon > 0$, and for $\varepsilon < 0$; (b) the real eigen wave $U(g, \bar{\zeta}_n^{\pm})$ in this case is 'something like leaky wave' (see for details work [2]). In the case $\mathrm{Re}\Gamma_n^{\pm}(\bar{\zeta}_n^{\pm}) = 0$, magnitudes $\mathrm{Im}\Gamma_n^{+}(\bar{\zeta}_n^{\pm})$ and $\mathrm{Im}\Gamma_n^{-}(\bar{\zeta}_n^{\pm})$ have the same sign for $\varepsilon < 0$ and different sign for $\varepsilon > 0$. This means that only in the case of a binegative medium filling the half-space $y < 0$, the real propagation constant $\bar{\zeta}_n^{\pm}$ can belong to a first (physical) sheet of the surface F_n and for such $\bar{\zeta}_n^{\pm}$ the relevant eigen wave $U(g, \bar{\zeta}_n^{\pm})$ is the real surface wave or 'true eigen wave' [2]. To implement such a possibility, it is sufficient (see the first of formulas (5)) that the inequality

$$\frac{\varepsilon\,(\varepsilon - \mu)}{\varepsilon^2 - 1} > 1 \quad \text{or} \quad \begin{cases} \varepsilon\mu < 1, & \text{if} \quad |\varepsilon| > 1 \\ \varepsilon\mu > 1, & \text{if} \quad |\varepsilon| < 1 \end{cases} \tag{6}$$

holds.

At small profiling depths of boundaries $\Sigma_x^{\varepsilon,\mu}$, the propagation constants corresponding to 'true eigen waves' $U(g, \bar{\zeta}_n^{\pm})$ branch off not far from the actual axis of the parameter variation $\zeta = kl/2\pi\beta$ [1, 5, 7]. In this case, we keep the same terms and identifiers for the corresponding spectral characteristics as in the case when $h = 0$. The approaching of ζ to one of the values $\bar{\zeta}_n^{\pm}$ causes anomalous (resonant) bursts in all characteristics describing diffraction radiation [1, 2, 5–7, 10]. It is now clear why we do not see such bursts in the case presented by Fig. 3.

Let's go back now to Figs. 1, 2, and discuss how the rapprochement of quantities $\zeta = kl/2\pi\beta$ and $\bar{\zeta}_n^{\pm}$ in the complex plane corresponding to the first (physical) sheet of the surface F (see [1, 2]) affects the specific characteristics $W_0^-(k,h)$ considered here. The resonance dip to zero of intensity of reverse VChR, which is clearly visible in Fig. 1(a), is associated with the excitation of the boundary's eigen wave, continuing at $h \neq 0$ the 'true eigen wave' $U(g, \bar{\zeta}_{-1}^{-})$ of plane boundary $y = 0$. Each such statement can be easily verified by calculating the corresponding values $\zeta = kl/2\pi\beta$ and $\bar{\zeta}_n^{\pm}$, and making sure they actually coincide. The Q-factors of the discussed resonances significantly decrease with the increase of h (Fig. 1(b)). This is obviously because the propagation constants of eigen waves corresponding to boundaries with a greater profiling depth move further in the complex plane from the real axis of the parameter ζ variation.

Peaks of the ridge I in Fig. 2 correspond to the excitation of 'true eigen waves' $U(g, \bar{\zeta}_{-2}^{-})$ and $U(g, \bar{\zeta}_1^{+})$, which complex propagation constants $\bar{\zeta}_{-2}^{-}$ and $\bar{\zeta}_1^{+}$ 'collide' on the real axis when value of $\zeta(k)$ approaches them (Fig. 4). That is why they are so sharp and high. It is possible that the maximum of the function $W_0^-(k,h) = 519.8$ that characterizes the VChR efficiency (see above) found here can be précised by decreasing the sampling step of the parameter k. The branches' 'collision' of the propagation

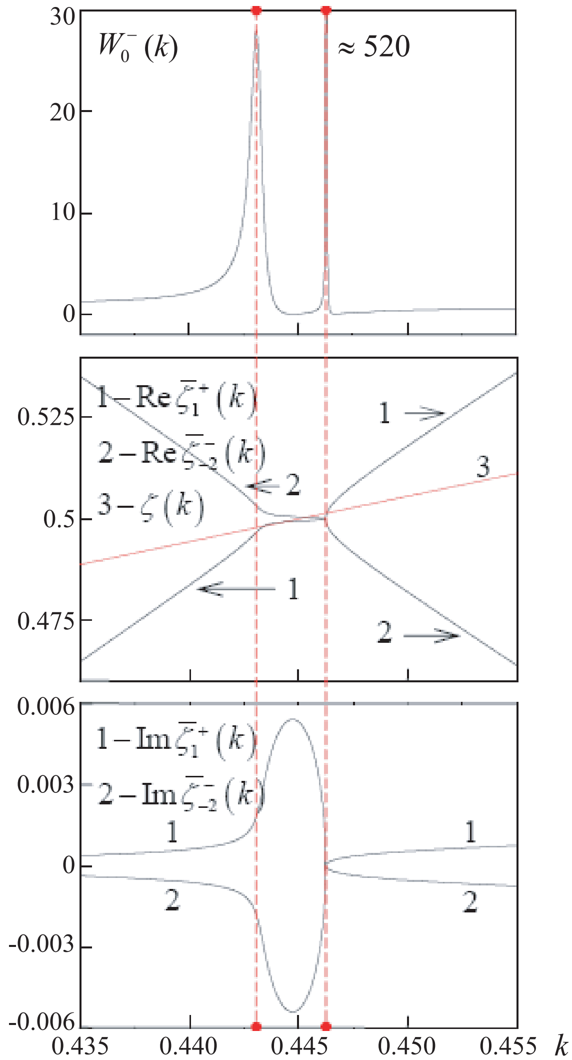

Figure 4. VChR intensity variation with reproaching of magnitude of $\zeta = kl/2\pi\beta$ and propagation constants $\bar{\zeta}_1^+$ and $\bar{\zeta}_{-2}^-$ of 'true eigen waves' of periodic interface: $h = 0.32$, $\mu(k) = -4.84$, $\varepsilon(k) = -0.84$, and $\beta = 0.89$.

constants of eigen waves of a periodic structure is a necessary condition for their transformation from 'complex' waves to 'real' waves and vice versa. In detail this phenomenon, whose one of the variants can be seen in Fig. 4, was discussed in [5, 7].

Peaks of the ridge II correspond to the excitation of 'true eigen wave' $U(g, \bar{\zeta}_1^+)$. The imaginary part of the propagation constant $\bar{\zeta}_1^+$ in modulus is much higher here (Fig. 4), and therefore the observed resonances do not have high Q-factor. This figure of merit decreases noticeably with an increase of h, and for the values $h \geq 0.75$ the considered resonance affects the behavior of the characteristic $W_0^-(k,h)$ not so noticeably.

In general, the data presented in Fig. 4 agree well with the conclusions from [5, 7, 11], where the foundations of the spectral theory of gratings as open periodic waveguides are outlined in details, and important conclusions are drawn about how the excitation of eigen waves in such structures affects their ability to implement various anomalous and resonant scattering modes of plane homogeneous and inhomogeneous waves.

The data presented in Fig. 5 allow to estimate the influence of parameters of the plasma-like medium k_ε and k_μ on the intensity of reverse VChR — here $\varepsilon(k) < 0$ and so the angle ϑ between the direction of

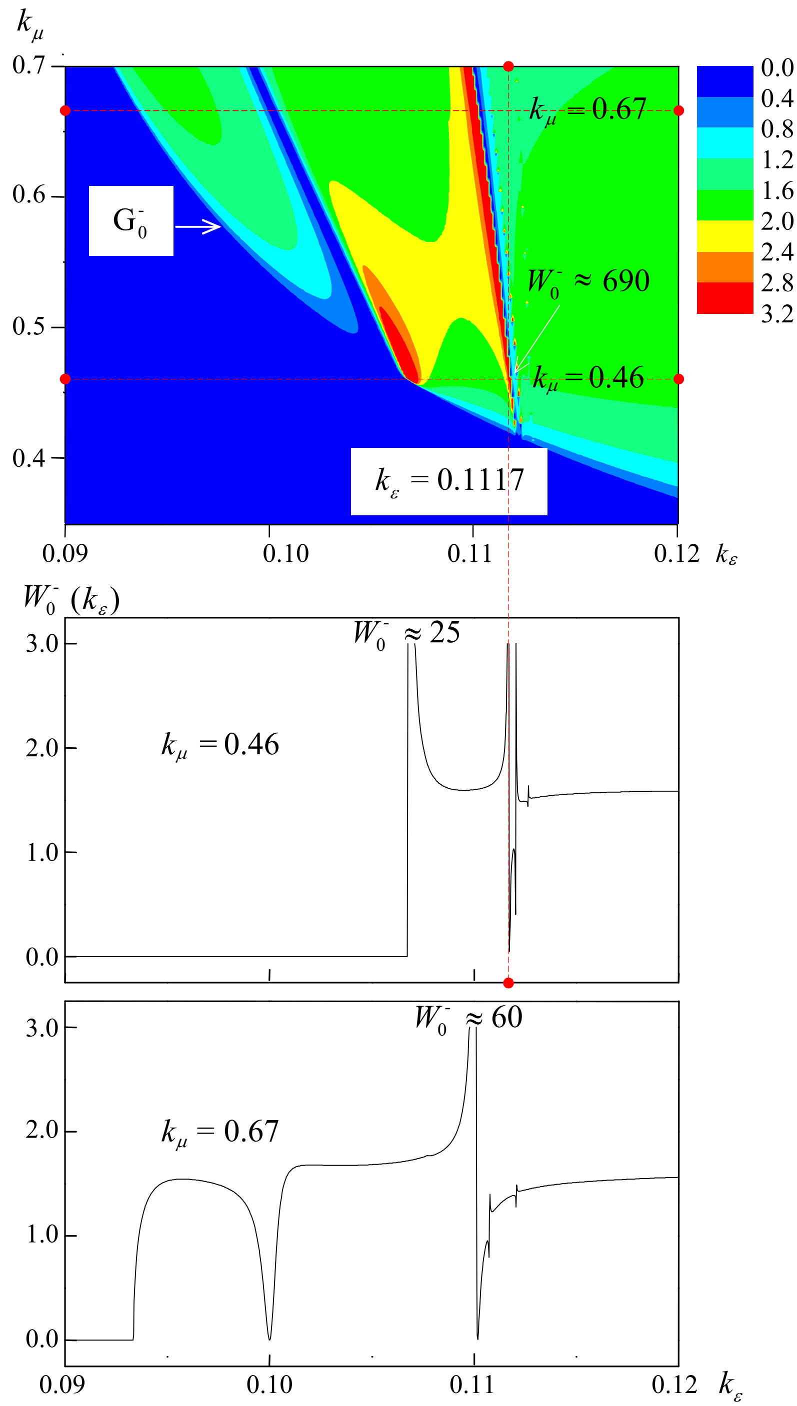

Figure 5. Efficiency $W_0^-(k_\varepsilon, k_\mu)$ of VChR in a half-space occupied by a binegative plasma-like medium, and a section of the surface $W_0^-(k_\varepsilon, k_\mu)$ by planes $k_\mu = 0.46$, $k_\mu = 0.67$: $h = 0.4$, $\beta = 0.2$, and $k = 0.08$.

the electron flow and the direction of energy transferring by the wave $U_0^-(g, k)$ is greater than $\pi/2$ [1].

The lines $W_0^-(k_\varepsilon, k_\mu) = const$ are calculated for parameters k_ε, k_μ from the domain $[0.09 \leq k_\varepsilon \leq 0.12] \times [0.35 \leq k_\mu \leq 0.7]$ and for $k = 0.08$, $\beta = 0.2$, and $h = 0.4$. Under such choice of parameters, the region bounded by the curve G_0^- is the domain of VChR. Here and further on, the curves $G_n^\pm = \{\ldots, \ldots\} : \Gamma_n^\pm(\ldots, \ldots) = 0$ are the boundaries separating the regions of parameters' variation corresponding the propagating spatial harmonics $U_n^{\pm}(g,k)$ and evanescent ones (see, for example, Fig. 4 in [2]).

Presented in Fig. 5 values W_0^- are cut off at the level $W_0^-(k_\varepsilon,k_\mu) = 3.0$, and $\max\limits_{k_\varepsilon,k_\mu} W_0^-(k_\varepsilon,k_\mu) \approx 690.6$ is achieved at values $k_\varepsilon = 0.1117$ (parameter k_ε sampling step is 0.00005) and $k_\mu = 0.46$ (parameter k_μ sampling step is 0.001). The first spike in the curve $W_0^-(k_\varepsilon)$ for $k_\mu = 0.46$ corresponds to a freestanding smoothed peak of the surface $W_0^-(k_\varepsilon,k_\mu)$ with a maximum height of 25.34 at the point $k_\varepsilon = 0.10675$. This peak, as well as the dip to zero values $W_0^-(k_\varepsilon,k_\mu)$ along the line to the left and above it, owes its existence to the excitation of the 'true eigen wave', with corresponding propagation constant $\bar{\zeta}_{-1}^-$ – here $Re\bar{\zeta}_{-1}^- \approx \zeta = 0.4$. A continuous ridge with high (from several tens to several hundred units) values of $W_0^-(k_\varepsilon,k_\mu)$ and a chain of free-standing peaks of surface $W_0^-(k_\varepsilon,k_\mu)$, occupying the place to the right of it, are located within a strip $0.1098 \leq k_\varepsilon \leq 0.1122$ adjacent to the value $k_\varepsilon = 0.1131$, for which the considered frequency k coincides with the singular point $k = \sqrt{0.5}k_\varepsilon = k^{\text{sing}}$ [2] that is a kind of 'accumulation' point of singularities: in the case of $k_\varepsilon > k_\mu$ and k approaching to k^{sing} from the left, and

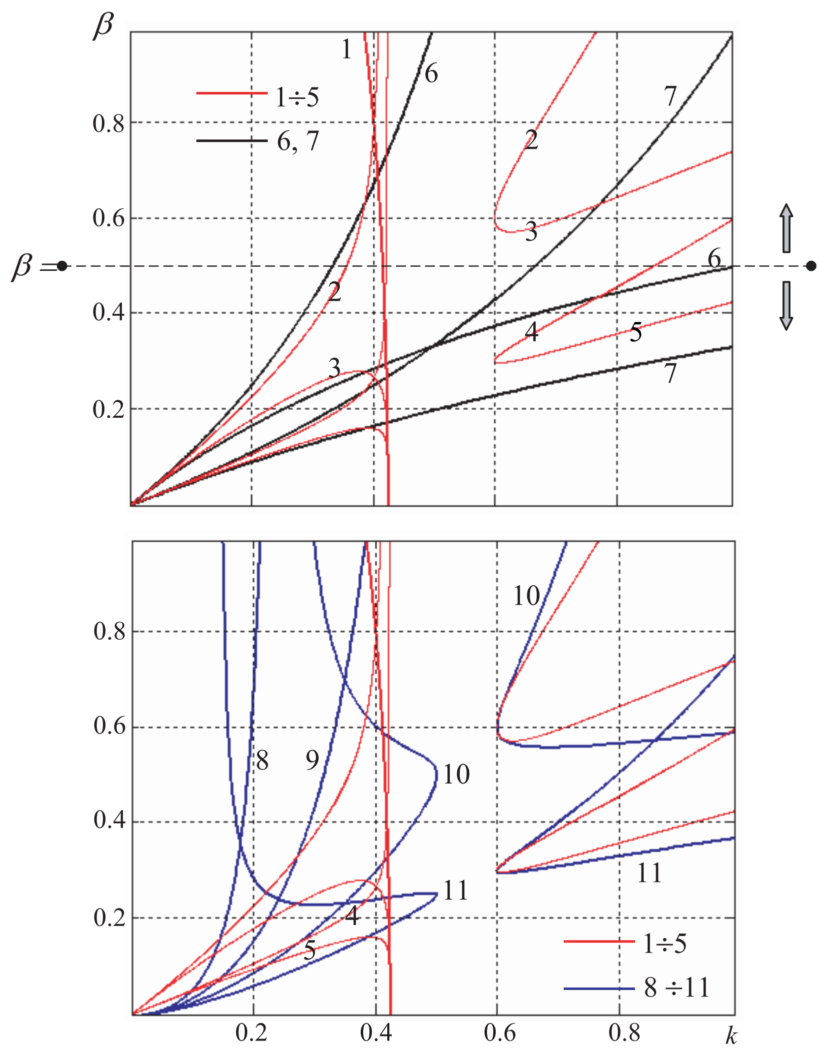

Figure 6. Boundaries $G_n^{\pm}$ in the domains of $k, \beta = kl/2\pi\zeta$ variation, separating regions where harmonics $U_n^{\pm}(g,k)$ propagate without attenuation; and dependences $\beta_n^{\pm}(k) = kl/2\pi\bar{\zeta}_n^{\pm}(k)$ for $\text{Im}\zeta_n^{\pm}(k) = 0, l = 2\pi, k_\varepsilon = 0.6\,(k^{\text{sing}} \approx 0.424)$ and $k_\mu = 0.5$: 1 — $\beta_0^+(k)$, 2 — $\beta_{-1}^-(k)$, 3 — $\beta_{-1}^+(k)$, 4 — $\beta_{-2}^-(k)$, 5 — $\beta_{-2}^+(k)$, 6 — G_{-1}^+, 7 — G_{-2}^+, 8 — G_1^-, 9 — G_0^-, 10 — G_{-1}^-, 11 — G_{-2}^-.

in the case of $k_\varepsilon < k_\mu$ and k approaching to k^{sing} from the right, we are faced with increasing number of the propagation constants $\bar{\zeta}_n^{\pm}(k)$ of 'unusual true eigen waves' $U(g, \bar{\zeta}_n^{\pm})$ [2]. That is why the number of high-Q resonances, causing a sharp drop and a sharp rise of $W_0^-(k_\varepsilon)$, increases here significantly.

The influence of profiling depth h on the intensity of VChR shows itself differently depending on the values of other parameters, and in fact, depending on whether a periodic boundary between two media at such values of parameters is able to support the propagation of 'unusual true eigen waves' $U(g, \bar{\zeta}_n^{\pm})$ [2] and whether the 'synchronization' $\text{Re}\,\bar{\zeta}_n^{\pm} \approx \zeta = kl/2\pi\beta$ of electron beam with these waves is possible.

3. SMITH-PURCELL RADIATION AND EIGEN MODES OF A PERIODIC INTERFACE

The radiation of $U_n^{\pm}(g, k)$, $n \neq 0$, harmonics propagating without attenuation in the domains $y > 0$ and $y < -h$, is Smith-Purcell radiation (SPR) [4, 5, 12, 13]. We have already touched upon the problem of the influence of eigen modes on the intensity of such radiation in [2]. Now we shall dwell on it in more detail, and the conclusions only outlined in [2] will be supported by the results of the relevant computing experiments. For their correct physical reading, information similar to that presented in Fig. 6, and information about the eigen waves $U(g, \bar{\zeta}_n^{\pm})$ of the periodic interface and their propagation constants $\bar{\zeta}_n^{\pm}$ given in [2] are of great importance.

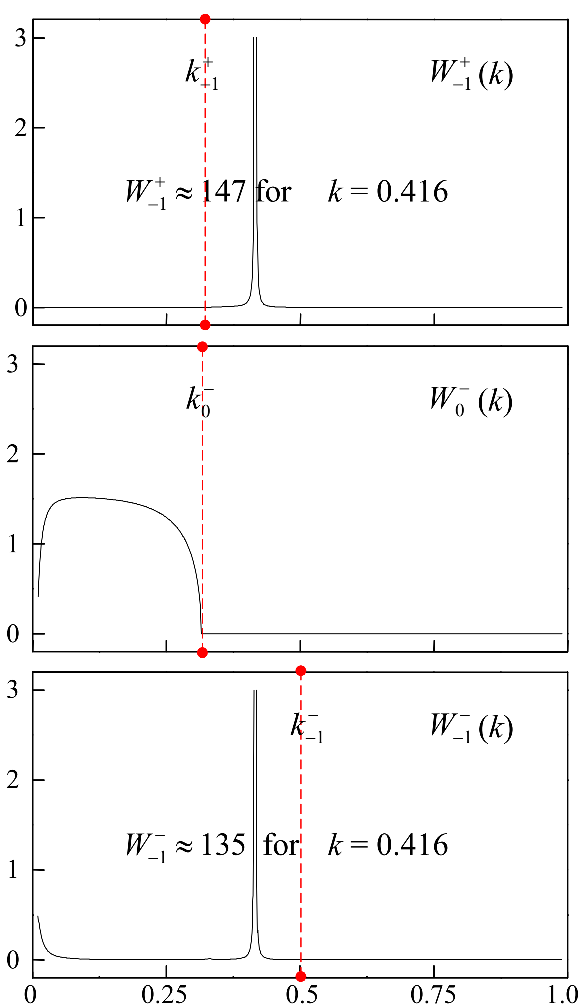

Figure 7. Intensity of SPR ($W_{-1}^{\pm}(k)$) and VChR ($W_0^-(k)$) for $\beta = 0.5$, $h = 0.1$, $k_\varepsilon = 0.6$ and $k_\mu = 0.5$.

So, Fig. 6 allows to reconstruct a general and fairly accurate qualitative picture of SPR for specific values k_ε, k_μ, and not very large h: by choosing a specific value $\beta = \ldots$, we obtain, for values k from the frequency range of interest, the information about the spatial harmonics $U_n^{\pm}(g, k)$ propagating here (about the harmonics at which diffraction radiation is carried out) and determine the frequencies k,

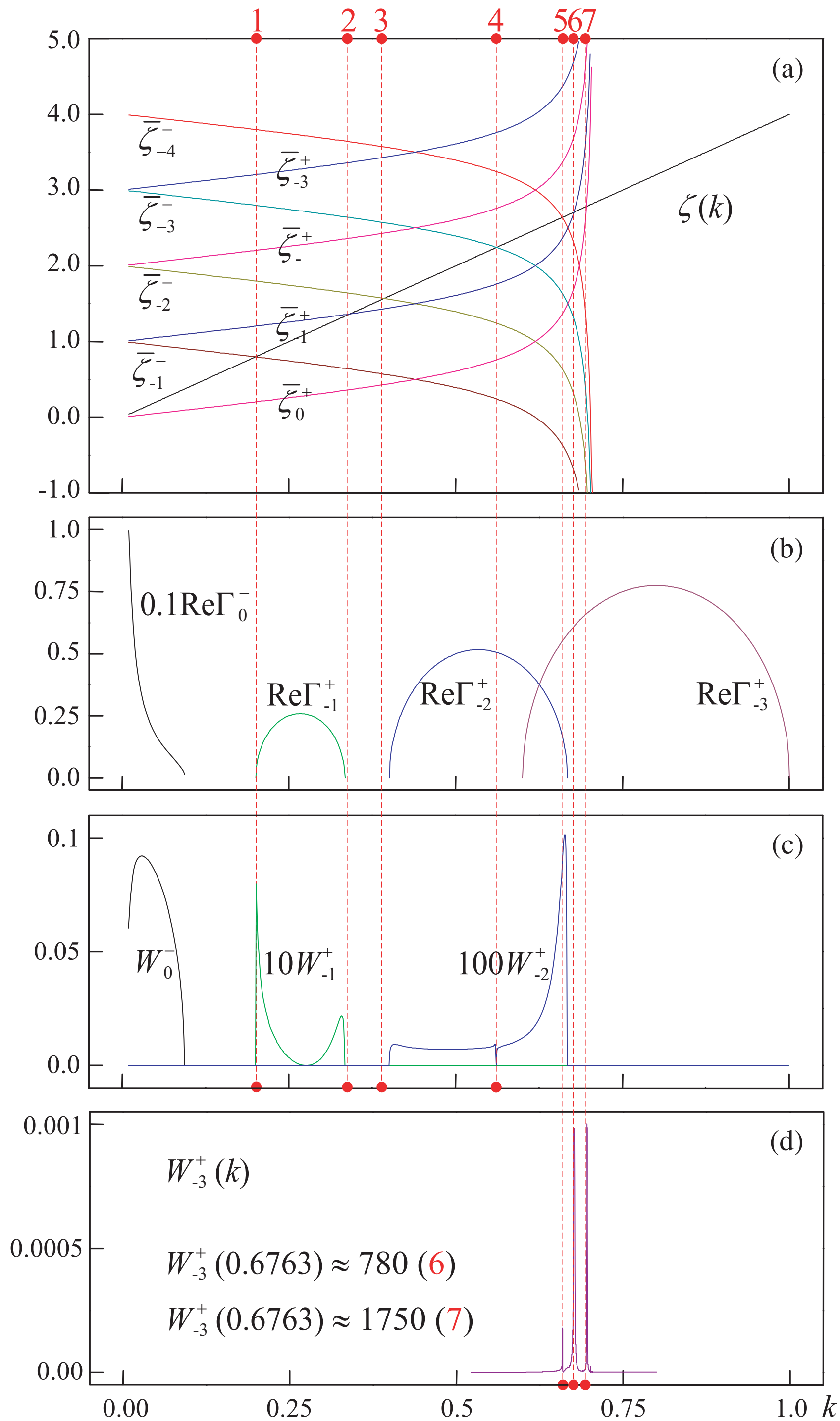

Figure 8. (a) Real valued propagation constants $\bar{\zeta}^{\pm}_{-}(k)$ of eigen waves $U(g, \bar{\zeta}^{\pm}_n)$ and function $\zeta(k)$, (b) values of $\mathrm{Re}\Gamma^{\pm}_n(k)$, (c) and (d) intensity of SPR ($W^{+}_{-m}(k)$, $m = 1, 2, 3$) and VChR ($W^{-}_0(k)$) : $k_\varepsilon = 1.0$, $k_\mu = 0.1$, $\beta = 0.25$ and $h = 0.2$.

providing the fulfilment of the condition $\bar{\zeta}_n^{\pm}(k) \approx \zeta(k)$; actually that are those values of k at which the straight line $\beta = \ldots$ intersects the curves $\beta_n^{\pm}(k)$. And at such values k the resonant modes of wave conversion are implemented, only if $\bar{\zeta}_n^{\pm}(k)$ lie on the first (physical) sheet of the surface F, which is a natural region of variation of the complex spectral parameter ζ [1, 2, 5–7].

Let $\beta = 0.5$. According to Fig. 6, the harmonic $U_{-1}^{+}(g,k)$ is a propagating one for frequency parameters $k > k_{-1}^{+} \approx 0.334$. Condition $\bar{\zeta}_n^{\pm}(k) \approx \zeta(k)$ holds in this domain in the vicinity of points $k \approx 0.355$ ($\bar{\zeta}_{-1}^{-}(k) \approx \zeta(k)$, $U(g, \bar{\zeta}_{-1}^{-})$ is the 'something like leaky wave'); $k \approx 0.416$ (in the vicinity of point k^{sing}, $\bar{\zeta}_0^{+}(k) \approx \zeta(k)$, $U(g, \bar{\zeta}_0^{+})$ is the 'unusual true eigen wave') and $k \approx 0.875$ ($\bar{\zeta}_{-2}^{-}(k) \approx \zeta(k)$, $U(g, \bar{\zeta}_{-2}^{-})$ is the 'something like leaky wave'). In the second case, the function $W_{-1}^{+}(k)$ reaches the value $W_{-1}^{+} \approx 147$ (the necessary and sufficient condition for the implementation of the resonance mode is fulfilled), and in the first and third cases ('synchronism' with 'something like leaky waves') the function $W_{-1}^{+}(k)$ remains at the same low level $W_{-1}^{+} < 10^{-1}$ as at all other points of the range $k > 0.334$ (see Fig. 7; the parameter step here is 0.001 and the values $W_{-1}^{\pm}(k)$ are 'cut' at level $W_{-1}^{\pm}(k) = 3.0$).

The function $W_{-1}^{-}(k)$ in the vicinity of the point $k \approx 0.416$ (here $W_{-1}^{-} \approx 135$) and in other points of the range $k < 0.5$, where the harmonic $U_{-1}^{-}(g,k)$ propagates without attenuation, behaves in the same way as the function $W_{-1}^{+}(k)$. The maximum radiation intensity at a harmonic $W_0^{-}(k)$ propagating without attenuation in the frequency range $k < k_0^{-} \approx 0.314$, which does not contain resonance points, is much lower and comparable to the corresponding values for the case of a flat interface [2].

In the case considered above, the frequency band $k_\varepsilon k_\mu (k_\mu^2 + k_\varepsilon^2)^{-1/2} < k < k^{\text{sing}}$ within which the propagation constant $\bar{\zeta}_n^{\pm}(k)$ of the 'unusual true eigen waves' can be detected [2] is very narrow ($0.384 < k < 0.424$). It adjoins directly to the point $k = k^{\text{sing}}$ and therefore it is practically impossible to accurately match any resonance with a precisely defined eigen wave. Let us expand this band to $0.1 < k < 0.707$, putting $k_\varepsilon = 1.0$, $k_\mu = 0.1$, and consider in detail how the 'synchronism' with the 'unusual true eigen waves' is related to the anomalous changes in the behavior of the functions $W_n^{\pm}(k)$ characterizing the efficiency of conversion of the field of the density modulated electron beam into the field of waves leaving the periodic interface (Fig. 8).

In Fig. 8 the frequencies meeting the conditions $\bar{\zeta}_n^{\pm}(k) \approx \zeta(k)$ are numbered: from the first to the seventh. The first two of them (here $\zeta(k) \approx \bar{\zeta}_{-1}^{-}(k)$ and $\zeta(k) \approx \bar{\zeta}_{-1}^{+}(k)$) are located near the cutoff points $k = k_{-1}^{+}$ of the spatial harmonic $U_{-1}^{+}(g,k)$ and the function $W_{-1}^{+}(k)$ reacts to this in a predictable way [1, 5–7]. In the immediate vicinity of the third point (here $\zeta(k) \approx \bar{\zeta}_{-2}^{-}(k)$), there are no propagating harmonics, and about the fifth (here $\zeta(k) \approx \bar{\zeta}_{-4}^{-}(k)$) can be said the same as about the first two, but now for the cutoff point $k = k_{-2}^{+}$ of the harmonic $U_{-2}^{+}(g,k)$. The fourth point (here $\zeta(k) \approx \bar{\zeta}_{-3}^{-}(k)$) falls into the middle of the range where the harmonic $U_{-2}^{+}(g,k)$ propagates without attenuation. Here 'synchronism' leads to a resonant fall to zero of the value of $W_{-2}^{+}(k)$, and as it is easy to see from Fig. 8(b), to the complete disappearance of diffraction radiation.

The points 6 and 7 (here $\zeta(k) \approx \bar{\zeta}_{-1}^{+}(k)$ and $\zeta(k) \approx \bar{\zeta}_0^{+}(k)$) are already close to the point $k = k^{\text{sing}}$, and the 'synchronism' corresponding to them leads to a fantastic increase in the energy capacity of the only harmonic $U_{-3}^{+}(g,k)$ propagating in the corresponding range: with the parameter k sampling step equal to 0.0001, the calculated levels of $W_{-3}^{+}(k)$ were $W_{-3}^{+}(k) \approx 780$ at $k = 0.6763$ and $W_{-3}^{+}(k) \approx 1750$ at $k = 0.6957$.

4. CONCLUSION

A plane, density-modulated electron beam, moving at a constant speed over an infinite one-dimensional periodic grating, generates homogeneous plane electromagnetic waves in the environment space. The number of waves, their wavelength, and direction of propagation are determined by the speed of the electron beam, its period of modulation and by the length of the period of grating. The same beam moving with a constant speed in a medium, where the speed of light is less than the speed of charged particles, generates in it two homogeneous plane electromagnetic waves, diverging from the direction of flow. The length of these waves and the direction of their propagation are determined by the period of beam modulation, the ratio of its velocity to the speed of light in the medium, as well as by the sign of the refractive index of the medium. The field of plane waves propagating above or below the grating or in a sufficiently optically dense medium is generated by the field of the charged particles flow.

This is how the processes that we today call coherent diffraction radiation or Vavilov-Cherenkov radiation [3, 14, 15] and Smith-Purcell radiation [4, 12, 13] are usually represented. The study of the relevant phenomena within the framework of such a concept has significantly enriched modern physics and made it possible to create a number of unique devices and systems of radio electronics and electronics of high power. The foundations were established for a reasonably rigorous mathematical modeling of diffraction radiation processes, which, in turn, made it possible to significantly expand the scope of the phenomena under the study due to the inclusion in them the so-called 'wave analogs of SPR and VChR' — the role of the intrinsic field of a beam of charged particles is played here by the field of an inhomogeneous plane wave or of a field of a surface wave directed by an open, for example, dielectric waveguide, and the polarization of this field can be arbitrary. New tasks, new results, and new opportunities for their practical use have appeared (see, for example, works [10, 16–22]).

The present work, continuing study [1, 2], presents new information about the possibility and conditions for the implementation of a number of anomalous and resonant phenomena in the processes of diffraction radiation generated by a density-modulated electron beam flying over a periodically uneven interface, in particular, over the periodic boundary separating vacuum and artificial dispersive medium. A detailed analysis of such phenomena can serve as a basis for the development of fundamentally new, accurate measuring schemes, e.g., diagnostic schemes and determination of intrinsic parameters of dispersive media and charged particle beams.

ACKNOWLEDGMENT

This research has been partially funded by the Science Committee of the Ministry of Education and Science of the Republic of Kazakhstan (Grant No. AP08855557).

REFERENCES

1. Sirenko, Y., S. Sautbekov, N. Yashina, and K. Sirenko, "Diffraction radiation generated by a density-modulated electron beam flying over the periodic boundary of the medium section. I. Analytical basis.*Progress In Electromagnetics Research B*, Vol. 91, 1–8, 2021.
2. Sirenko, Y., S. Sautbekov, N. Yashina, and K. Sirenko, "Diffraction radiation generated by a density-modulated electron beam flying over the periodic boundary of the medium section. II. Impact of true eigen waves," *Progress In Electromagnetics Research B*, Vol. 91, 9–17, 2021.
3. Cherenkov, P., "Visible radiation produced by electrons moving in a medium with velocities exceeding that of light," *Physical Review*, Vol. 52, 378–379, 1937.
4. Smith, S. and E. Purcell, "Visible light from localized surface charges moving across a grating," *Physical Review*, Vol. 92, No. 4, 1069–1073, 1953.
5. Shestopalov, V. and Y. Sirenko, *Dynamic Theory of Gratings*, Naukova Dumka, Kiev, 1989 (in Russian).
6. Sirenko, Y. and S. Strom (eds), *Modern Theory of Gratings. Resonant Scattering: Analysis Techniques and Phenomena*, Springer, New York, 2010.
7. Shestopalov, V. and Y. Shestopalov, *Spectral Theory and Excitation of Open Structures*, The Institution of Electrical Engineers, London, 1996.
8. Shestopalov, V., A. Kirilenko, S. Masalov, and Y. Sirenko, *Resonance Wave Scattering. Vol. 1. Diffraction Gratings*, Naukova Dumka, Kiev, 1986 (in Russian).
9. Sirenko, Y., "Analytical extension of diffraction problems and threshold effects in electromagnetics," *Doklady Akademii Nauk Ukrainskoy SSR, Seriya A*, No. 8, 65–68, 1986 (in Russian).
10. Sautbekov, S., K. Sirenko, Y. Sirenko, A. Poyedinchuk, N. Yashina, and A. Yevdokymov, "Smith-Purcell effect. Anomalously high level of outgoing wave excitation," *Telecommunications and Radio Engineering*, Vol. 77, No. 6, 469–487, 2018.

11. Sirenko, Y., "A grating in the field of a compact monochromatic source," *Electromagnetics*, Vol. 13, No. 3, 255–272, 1993.
12. Bolotovskiy, B. and G. Voskresenskiy, "Radiation of charged particles in periodic structures," *Uspehi Fizicheskih Nauk*, Vol. 94, No. 3, 378–416, 1968 (in Russian).
13. Shestopalov, V., *The Smith-Purcell Effect*, Nova Science Publishes, New York, 1998.
14. Jelley, J., *Cherenkov Radiation and Its Applications*, Pergamon Press, London, 1958.
15. Frank, I., *Vavilov-Cherenkov Radiation*, Nauka, Moscow, 1988 (in Russian).
16. Kesar, A., "Smith-Purcell radiation from a charge moving above a grating of finite length and width," *Physical Review Special Topics — Accelerators and Beams*, Vol. 13, 022804-1–022804-8, 2010.
17. Burlak, G. "Spectrum of Cherenkov radiation in dispersive metamaterials with negative refraction index," *Progress In Electromagnetics Research*, Vol. 132, 149–158, 2013.
18. Sautbekov, S., K. Sirenko, Y. Sirenko, and A. Yevdokimov, "Diffraction radiation phenomena: Physical analysis and applications," *IEEE Antennas and Propagation Magazine*, Vol. 57, No. 5, 73–93, 2015.
19. Granet, G., P. Melezhik, A. Poyedinchuk, S. Sautbekov, Y. Sirenko, and N. Yashina, "Resonances in reverse Vavilov-Cherenkov radiation produced by electron beam passage over periodic interface," *International Journal of Antennas and Propagation*, Vol. 2015, 10p., 2015.
20. Sirenko, Y. and L. Velychko, (eds), *Electromagnetic Waves in Complex Systems: Selected Theoretical and Applied Problems*, Springer, New York, 2016.
21. Melezhik, P., M. Ney, S. Sautbekov, K. Sirenko, Y. Sirenko, A. Vertiy, and N. Yashina, "Cherenkov radiation based antenna with the funnel-shaped directional pattern," *Electromagnetics*, Vol. 38, No. 1, 34–44, 2018.
22. Sautbekov, S., K. Sirenko, Y. Sirenko, and A. Yevdokymov, "Diffraction antennas. Synthesis of radiating elements," *Telecommunications and Radio Engineering*, Vol. 77, No. 11, 925–943, 2018.